Astron. Astrophys. 325, 1264–1279 (1997)

ASTRONOMY
AND
ASTROPHYSICS

Chemical reactions in protoplanetary accretion disks

II. Carbon dust oxidation

F. Finocchi[1], **H.-P. Gail**[1], **and W. J. Duschl**[1,2]

[1] Institut für Theoretische Astrophysik, Universität Heidelberg, Tiergartenstraße 15, D-69121 Heidelberg, Germany
[2] Max-Planck-Institut für Radioastronomie, Auf dem Hügel 69, D-53121 Bonn, Germany

Received 6 November 1996 / Accepted 27 January 1997

Abstract. This paper considers the gas phase chemistry in a protoplanetary accretion disk, especially the chemistry initiated in the gas phase by destruction of dust close to the central star.

Slow radial particle transport moves gas and dust from the cold outer parts of a protoplanetary accretion disk into its warm central part where chemical reactions in the gas phase are activated. At the same time gases frozen on the surface of dust grains are vaporized and later the dust grains themselves are vaporized or destroyed by chemical surface reactions. In this paper we take into account oxidation processes of carbon dust by OH molecules and free O atoms. Oxidation by OH molecules turns out to be very efficient and strongly modify the hydrocarbon chemistry in the protoplanetary disk. Due to the slow conversion of hydrocarbons to CO at low temperatures we find that large amounts of methane and more complex organic molecules are formed in the region between the present positions of Venus and Mars. Closer to the protosun, these are converted into CO.

Key words: accretion disks – molecular processes – solar system: formation

1. Introduction

The generally accepted model for stellar and solar system formation is the collapse of a rotating molecular cloud. The centrifugal forces lead to the formation of a flat structure, a *protostellar accretion disk*. Most of the infalling material is first incorporated into this disk and then moves inwards and finally becomes part of the newly forming star. This inwards directed accretion of the matter in the disk is due to some kind of viscous process probably generated by turbulent motions.

The evolution of a protostellar accretion disk can be divided into three distinct phases (Cameron 1988):

Send offprint requests to: H.-P. Gail,
(gail@phyllis.ita.uni-heidelberg.de)

During the first stage of formation, the protoplanetary disk is built up by infalling matter from the surrounding molecular cloud. This phase lasts for about 10^5 years.

In the second phase, the external supply of mass has nearly ceased and most of the mass is concentrated in the young central star. The protoplanetary disk is now formed: a thin disk of matter revolving at nearly the local Keplerian velocity around the protosun. In this disk most of the material drifts inwards while angular momentum is transported outwards causing the disk to spread out (Lynden-Bell and Pringle 1974). The mass of the disk itself is small compared to the central mass and the disk is geometrically thin. A characteristic time scale for the duration of this stage is the viscous time scale, which is $\approx 10^5 \ldots 10^6$ years. In this viscous stage, the formation of planetary bodies due to the agglomeration of dust particles in the middle plane of the accretion disk is possible.

During the third and last stage, the gaseous component (mostly the light elements) of the accretion disk is dispersed, probably by the action of the powerful bipolar stellar wind of the central star in its T Tauri phase. T Tauri stars are the first optically visible stage during formation process of low-mass stars. The heavier metallic elements can be present as newly formed planetary bodies: a solar system, then, is born. The duration of this last phase could be somewhat longer ($\approx 10^7$ years, e.g. Beckwith and Sargent 1993).

In this paper we consider the second stage (the viscous phase) of the accretion disk evolution and calculate the chemical composition of the disk material from the reaction kinetics of the gas phase in the disk's middle plane from the outermost edge of the disk down to a position close to the transition layer between the disk and the protosun. Although the prospects for probing the chemical compositions of accretion disks around young stars are extremely dim at present, the chemical evolution of the disk material in this stage is of fundamental importance for understanding the formation of planetary systems in general, and of our own Solar System in particular. For this we consider a gas parcel drifting inwards to the disk's center. The chemistry in this particular parcel is calculated by solving numerically an extended chemical reactions network for the gas

phase chemistry, the vapourisation and chemical destruction of dust grains together with a semi-analytical model for the structure of the accretion disk in a one-zone approximation (in the vertical direction).

The resulting differential-algebraic system is extremely stiff and highly non linear, mainly because of the exponential temperature dependence of the rate coefficients and the close coupling between chemistry and temperature structure in the disk. The equations are solved by using the powerful integrator DAESOL (Bleser 1986, Eich 1987, Bauer 1994) which in our previous work (Bauer et al. 1996, hereafter called Paper I) turned out to be very efficient for this kind of problems.

The plan of this paper is as follows: In Sect. 2 we briefly describe the disk model on which our calculation is based and our approximation for the gas opacity. Section 3 presents the equations of the gas phase chemistry and the chemical network. In Sect. 4 we describe our model for the dust and the ices, their vapourisation and destruction. Our results and interpretations are given in Sect. 5. The results are summarised in Sect. 6.

2. Model of the accretion disk

We use in this paper the same semi-analytical model for a thin stationary accretion disk as in Duschl et al. (1996, henceforth called Paper II)[1] and in Paper I. The details of the model are described in Paper II. The resulting basic equations for the disk structure are

$$\Sigma = 2500 \frac{\mathrm{g}}{\mathrm{cm}^2} s^{-\frac{3}{5}} \quad (1)$$

$$h = 1.446 \cdot 10^{12} \mathrm{cm}\ s^{\frac{21}{20}} \left(\frac{M}{M_\odot}\right)^{-\frac{3}{8}} \left(\dot{\mathbf{M}}_{-7}\,\kappa\right)^{\frac{1}{8}} \mu^{-\frac{1}{2}} \quad (2)$$

$$T = 997\ \mathrm{K}\ s^{-\frac{9}{10}} \left(\frac{M}{M_\odot}\right)^{\frac{1}{4}} \left(\dot{\mathbf{M}}_{-7}\,\kappa\right)^{\frac{1}{4}} \quad (3)$$

$$P = 71.65 \frac{\mathrm{g}}{\mathrm{cm\ s}^2} s^{-\frac{51}{20}} \left(\frac{M}{M_\odot}\right)^{\frac{5}{8}} \left(\dot{\mathbf{M}}_{-7}\kappa\right)^{\frac{1}{8}} \mu^{-\frac{1}{2}} \quad (4)$$

where s is the radial distance from the protosun in units AU, Σ is the surface density, h the (half) thickness of the disk, M the mass of the protostar, $M_\odot$ the solar mass, $\dot{\mathbf{M}}_{-7}$ the constant accretion rate in units of $\dot{\mathbf{M}}/(10^{-7}\ M_\odot/\mathrm{yr})$, and P and T are the pressure and temperature in the midplane of the disk, respectively. κ is the mass absorption coefficient and μ the mean molecular weight. The opacity is determined by the opacity of the dust and the gas (see Sect. 2.1).

Illumination due to the accreting star and/or the disk-star boundary layer may lead to modifications of the disk structure, even to self induced warping (Pringle 1996). In the present investigation such effects are not accounted for.

The inwards directed drift velocity of the disk material is

$$v_s = 26.94 \frac{\mathrm{cm}}{\mathrm{s}} s^{-\frac{2}{5}} \dot{\mathbf{M}}_{-7}\,. \quad (5)$$

[1] In the printed version of Paper II the dot over $\dot{M}$ denoting the mass-loss rate is missing in all equations. The correct version may be obtained from the WWW

Table 1. Model parameters of the accretion disk used in the computation of disk structure

mass M	$1\,M_\odot$
mass-loss rate $\dot{\mathbf{M}}$	$10^{-7}\,M_\odot/\mathrm{yr}$
surface density Σ	2500 g·cm^{-2} at $s = 1$

Integrating this with respect to time yields the radial position of a fixed gas parcel at each instant t

$$s^{1.4} = s_0^{1.4} - 2.52 \cdot 10^{-12} \dot{\mathbf{M}}_{-7}\, t\,. \quad (6)$$

s_0 is the initial position of the parcel at $t = 0$.

The vertical component v_z of the gas velocity accounting for the decrease of the height h of the accretion disk with decreasing s is

$$v_z = \frac{dh}{dt} = \frac{dh}{ds}\frac{ds}{dt} = -\frac{dh}{ds} v_s\,. \quad (7)$$

In the one zone approximation, the vertically averaged gradient of the vertical velocity is

$$\frac{\partial v_z}{\partial z} \approx \frac{v_z}{h}\,. \quad (8)$$

The basic parameters of the disk model used in our calculation are listed in Table 1.

2.1. Opacity

In our model calculation, the opacity of the disk material is determined for each time step simultaneously with the temperature in the central plane of the disk. The temperature dependent Rosseland mean opacity of the two main dust components (silicate and graphite) is calculated using the dust extinction model of Draine and Lee (1984) and Draine (1985) (see Paper I for more details). This is probably a strong oversimplification for the true absorption properties of dust in protoplanetary accretion disks since coagulation will modify the dust properties (e.g. Henning and Stognienko 1996), but this process presently cannot be coupled to our type of model calculation.

For the Rosseland mean of the mass extinction coefficient of the gas, κ_{gas}, we use the analytical approximations to tabular values given by Lin and Papaloizou (1985) and Bell and Lin (1994):

(i) Once the whole dust has disappeared, the absorption is dominated by molecules (mainly H_2O and TiO, see for instance the Figs. in Alexander 1975 or Sharp 1992). In the region where molecular extinction dominates the mass extinction coefficient of the gas can be approximated by

$$\kappa_{\mathrm{mol}} = 1.0\,10^{-8} \cdot \rho^{\frac{2}{3}} \cdot T^3 \quad [\mathrm{cm}^2/\mathrm{g}]\,. \quad (9)$$

(ii) In the temperature regime between $\approx$ 4 000 K and $\approx$ 10 000 K the H^- ions dominate the extinction. In this region the mass extinction coefficient can be approximated by

$$\kappa_{\mathrm{H}^-} = 1.0\,10^{-36} \cdot \rho^{\frac{1}{3}} \cdot T^{10} \quad [\mathrm{cm}^2/\mathrm{g}]\,. \quad (10)$$

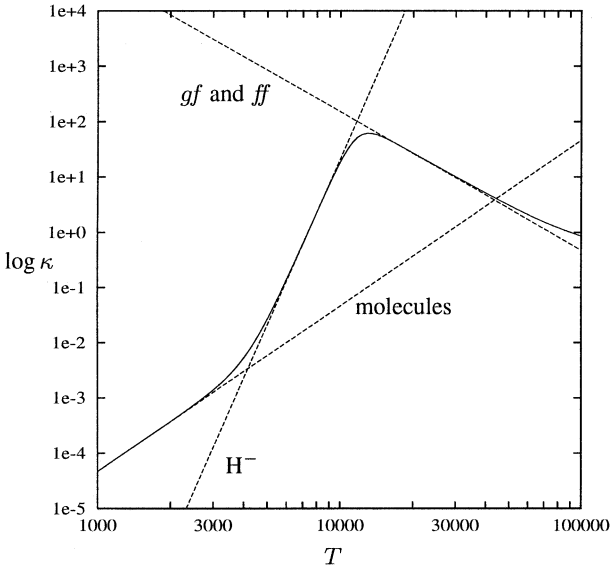

Fig. 1. Interpolation of the extinction coefficient. The dashed curves show the extinction by the indicated opacity sources for a mass density of $\rho = 1 \cdot 10^{-8}\,\mathrm{g/cm^3}$. The full line is the interpolated extinction coefficient according to the prescription (12).

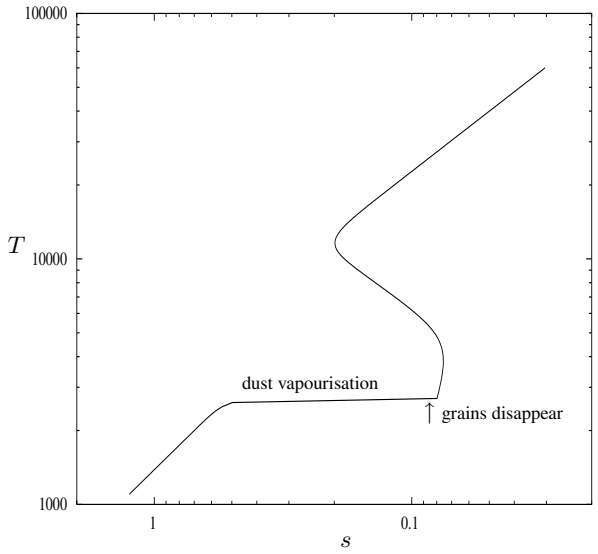

Fig. 2. Structure of a stationary accretion disk with opacity law (12) for the gas component.

We note the high power of the temperature in this case: a small change in the temperature dramatically modifies the opacity. This strong temperature dependence of κ is the cause of the so called *viscous instability* in accretion disks. Test calculations for the time evolution of a protoplanetary disk using this opacity law, indeed, showed this type of instability triggered by the steep temperature raise of κ to occur (cf. Bell and Lin 1994).

(iii) For higher temperatures *gf* and *ff* transitions of atoms and ions dominate the extinction of the gas. The mass extinction coefficient can be approximated in this case by

$$\kappa_{\mathrm{gf}} = 1.5\,10^{20} \cdot \rho \cdot T^{-\frac{5}{2}} \quad [\mathrm{cm^2/g}]\,. \tag{11}$$

Temperatures above $\approx 10^4\,\mathrm{K}$ where this approximation becomes valid are usually not encountered in a protoplanetary accretion disk. For our set of accretion disk parameters (cf. Table 1) such high temperatures occur only at the smallest radii of the disk (Eq. 3) and in the transition layer to the stellar surface. Our model approximations for the disk break down in this transition zone (see, e.g., Duschl and Tscharnuter 1991).

The total gas opacity is calculated from the interpolation formula

$$\kappa_{\mathrm{gas}}^{-1} = [\kappa_{\mathrm{mol}} + \kappa_{\mathrm{H^-}}]^{-1} + \kappa_{\mathrm{gf}}^{-1} \tag{12}$$

which smoothly interpolates between the different cases. In Fig. 1 the different opacity approximations are displayed for a value of the mean density of $10^{-8}\,\mathrm{g{\cdot}cm^{-3}}$ together with the interpolated value of the total opacity. The total mass extinction coefficient of the disk material (dust + gas) finally is obtained by the simple summation

$$\kappa = \kappa_{\mathrm{gas}} + \kappa_{\mathrm{dust}} = \kappa_{\mathrm{gas}} + \frac{\rho_s}{\rho}\kappa_s + \frac{\rho_c}{\rho}\kappa_c\,. \tag{13}$$

ρ_s and ρ_c are the mass density of the carbon and silicon dust in the gas-dust mixture and κ_s and κ_c are their extinction coefficients. This simple addition of the different opacities is surely not very precise but it should be sufficient for our present more explorative calculation.

Fig. 2 shows as an example the temperature structure in the inner part of the disk for $s \lesssim 1$ AU resulting from this opacity law. The dust vapourisation and the dissociation are calculated here not by solving the corresponding rate equations but from thermodynamic equilibrium as in Paper II. The disk equations with the opacity law (13) have multiple valued solutions for T and P in the radius interval $0.186\,\mathrm{AU} < s < 0.0728\,\mathrm{AU}$ which results from the steep increase of opacity in the region of hydrogen dissociation. If one starts at large s and moves inwards one first moves on the lower branch of the solution into the multiple valued region. In the stationary case there results a strong upwards jump in the temperature if one reaches the lower critical radius s_c at 0.0728 AU where dT/ds becomes singular. As one moves further inwards the solution then continues on the high temperature branch.

For time dependent models of an accretion disk it is known that the very strong temperature dependence of the $\mathrm{H^-}$ opacity ($\propto T^{10}$, Eq. 10), resulting in the multi-valued solution for the stationary case, gives rise to an unstable structure of the disk (Meyer and Meyer-Hofmeister 1981, Duschl 1991). This instability, however, is not destructive to the disk but rather gives rise a limit-cycle behaviour. This introduces an inherent time dependence into the problem and thus leads beyond the scope of our present work. While the basic features of the instability and the time dependent disk evolution due to it have been investigated and are understood fairly well, not very much is known how a proper treatment of the chemical evolution influences the overall evolution of such an unstationary accretion disk. In this context it is important to note that not only steep opacity gradients due

to hydrogen ionisation/recombination can give rise to an instability. Also steep gradients due to destruction of molecular absorbers (e.g., H_2O) can lead to similar consequences. We will address the question of the chemical evolution of unstationary accretion disks in a forthcoming paper.

In the present models of the chemistry of the disk we perform the inwards integrations of the rate equations only down to a radius slightly above the critical radius at $s \approx 0.073$ AU where the solution of the disk equations becomes singular. The calculation is stopped at this point since the high temperature branch of the solution is of no interest for the chemistry.

The opacity law (13) is used to determine for each time step the temperature from Eq. (3) and pressure from Eq. (4) which is equivalent to determine the zeros of the two following functions F and G:

$$F(P,T) \equiv T - 997\, s^{-\frac{9}{10}} \left(\frac{M}{M_\odot}\right)^{\frac{1}{4}} (\dot{\mathbf{M}}_{-7})^{\frac{1}{4}}\, \kappa^{\frac{1}{4}}(P,T) \qquad (14)$$

$$G(P,T) \equiv P - 71.65\, s^{-\frac{51}{20}} \left(\frac{M}{M_\odot}\right)^{\frac{5}{8}} (\dot{\mathbf{M}}_{-7})^{\frac{1}{8}}\, \frac{\kappa^{\frac{1}{8}}(P,T)}{\mu^{\frac{1}{2}}(P,T)}\,. \qquad (15)$$

The extremely non-linearity of these functions results in considerable numerical problems if coupled to the system of rate equations for the chemistry and dust destruction, but the numerical method presented in Paper I is well suited to handle such problems.

3. Chemistry in the accretion disk

As in Paper I we consider that the chemistry in a protoplanetary accretion disk in the outer parts of the disk operates far away from thermodynamic and chemical equilibrium. A kinetical treatment of the possible reaction pathways is necessary in this case. We consider explicitly the reaction kinetics in the gas phase and the dust related processes of vapourisation and chemical sputtering.

3.1. Assumptions

The generally low particle density in an accretion disk as compared to laboratory conditions allows one to restrict the gas phase chemistry essentially to binary reactions between neutral atomic and molecular species only. The only exceptions are ternary reactions between the abundant hydrogen particles H and H_2 and ternary reactions involving He for which we included the corresponding three-body association reactions. Though H_2 formation by this mechanism is generally inefficient under astrophysical conditions, it becomes important in an accretion disk due to the long available accretion timescale $\tau_{\rm accr} = |s/v_s| \approx 10^4$ yr and rather high particle densities.

We neglect the possibility of ionisation or dissociation by UV radiation from the central star because in the viscous phase the disk is optically thick in the radial and vertical directions. Such photo-dissociations and the ion-molecule chemistry driven by photoionisation are probably important in the optically thin outer atmospheric layers of the disk which may be illuminated either directly by the central star or indirectly by scattered starlight. This problem can adequately be treated only on the basis of a vertically stratified model including vertical mixing processes, which is beyond the present computational possibilities. We can make, however, the following qualitative estimation: The mass absorption coefficient of the gas-dust mixture in the short wavelength region is of the order of $1 \ldots 10\,\mathrm{cm^2 \cdot g^{-1}}$. The ionising radiation then penetrates only into a depth corresponding to a mass surface density of the order of $1 \ldots 0.1\,\mathrm{g \cdot cm^{-2}}$. The surface density of the layer for which the photochemistry may be important is, thus, very small compared to the surface density Σ of the protoplanetary accretion disk over the whole extension of the present planetary system (cf. Eq. (1)). It seems unlikely, then, that such processes can really affect the chemistry in the midplane of the disk, in which we are mainly interested, since only a very small fraction of the total mass contained in the optically thin outer layers is involved in such photoprocesses.

Another source of ionisation are the ever present cosmic rays. They are stopped and absorbed on a length corresponding to a mass surface density of $\approx 200\,\mathrm{g \cdot cm^{-2}}$. The surface density Σ of the accretion disk in the region of the terrestrial planets is of the order of several $10^3\,\mathrm{g \cdot cm^{-2}}$. Thus, in the inner region of the protoplanetary accretion disk the cosmic rays cannot penetrate deeply into the accretion disk. The ion-molecule chemistry driven by cosmic ray ionisation only affects a thin surface layer of the disk and, again, it seems unlikely that this affects the chemistry in the midplane of the disk. This also holds for X-rays emitted from the T Tauri wind region. The thickness of this layer, however, much exceeds the thickness of the layer for which the photochemistry may be important. From (1) we find that $\Sigma(s)$ drops to a value of $\approx 200\,\mathrm{g \cdot cm^{-2}}$ at a distance of $s \approx 70$ AU. In the outermost region of the protoplanetary accretion disk the cosmic rays penetrate deeply into the disk and may substantially modify the chemistry in this part of the disk. Presently, this ionisation is not included in the calculation since in this paper we are interested in the basic chemical processes in the protoplanetary disk triggered by dust destruction in the region of the terrestrial planets.

A third source of ionisation are the extinct radio nuclides, i.e. unstable nuclides with half lifes of the order of 0.1 to 100 Myr which have all decayed since the formation of our planetary system 4.8 Gyr ago. Such nuclei have been present in the early solar system as we know from studies of the isotopic composition of pristine material from our solar system found in certain meteorites (cf. Wasserburg 1985, Swindle 1993). The most important source of ionisation by such extinct radio nuclides was the decay of ^{26}Al. The ionisation rate by ^{26}Al was calculated by Umebayashi and Nakano (1981) and seems to be slightly less than that of the cosmic rays, but this source of ionisation is not shielded by overlying matter as in the previous two cases since these nuclei are part of the matter in the accretion disk. We have not included this process in the present calculation for the same reason as above.

In the innermost part of the disk at temperatures above $\approx$ 3 000 K the abundant elements of low ionisation potential start to be ionised either by collisional or radiative processes. These

processes also are not included in this calculation. All these ionisation processes and the resulting ion–molecule chemistry will be discussed in a forthcoming paper (Finocchi et al. 1997). In this paper we consider the neutral-neutral chemistry only, which dominates the chemistry in the region of the terrestrial planets and the dust destruction.

3.2. Equations for the gas-phase chemistry

The basic equation governing the time evolution of a specific atomic or molecular species is the continuity equation

$$\frac{\partial n_i}{\partial t} + \nabla \cdot (n_i \boldsymbol{v}) = R_i \,. \tag{16}$$

n_i is the particle density of the considered species, $\boldsymbol{v}$ is the velocity and R_i denotes the chemical source and sink terms. The most appropriate coordinate system for the description of the accretion disk is the cylindrical one. If s is the radial distance from the protosun, z the vertical height over the midplane of the disk, and if we assume rotational symmetry with respect to the z-axis, the change of n_i along a streamline is

$$\frac{\mathrm{d}n_i}{\mathrm{d}t} = \frac{\partial n_i}{\partial t} + v_s \frac{\partial n_i}{\partial s} + v_z \frac{\partial n_i}{\partial z} \,. \tag{17}$$

Then (16) simplifies to the following ordinary differential equation for n_i in a comoving frame

$$\begin{aligned} \frac{\mathrm{d}n_i}{\mathrm{d}t} \;=\; & -n_i \left(\frac{v_s}{s} + \frac{\partial v_s}{\partial s} + \frac{\partial v_z}{\partial z} \right) \\ & -n_i \sum_j k_{ij} \cdot n_j + \sum_{jl} k_{ijl} \cdot n_j \cdot n_l \\ & -n_i \sum_{jl} k'_{ijl} \cdot n_j \cdot n_l + \sum_{jlm} k_{ijlm} \cdot n_j \cdot n_l \cdot n_m \,. \end{aligned} \tag{18}$$

The k_{ij}, k_{ijl} are the rate coefficients of the sink and source terms of binary gas phase reactions, and k'_{ijl} and k_{ijlm} are the rate coefficients of the sink and source terms of ternary gas phase reactions, respectively. In the one-zone approximation for the thin accretion disk Eq. (18) is averaged with respect to the z-dependence. n_i and the rate coefficients then are replaced by their values in the midplane of the disk. The averaged v_s is given by (5) and the averaged z-gradient of v_z is given by (8).

These rate coefficients $k_{\ldots}$ are approximated by the standard Arrhenius form

$$k = k_0 T^{\alpha} \exp\left(-\frac{E_a}{kT} \right) \,. \tag{19}$$

k_0 and α are constants and E_a is the activation energy barrier.

In principle Eq. (18) has to be complemented by a term describing the infall of matter from the surrounding molecular cloud. In the viscous stage of the evolution of the protoplanetary disk it is assumed that the infall has more or less ceased and, for this reason, we have neglected such source terms in our model calculation. There is some observational indication, however, that there is continued infall of matter at a low rate ($\lesssim 10^{-7}\, M_\odot/\,\mathrm{yr}$) even in the T Tauri phase (van Langenvelde et al. 1994, Bontemps et al. 1996)). This is probably important for the chemistry in the disk since the infall will feed fresh, chemically unprocessed material into the disk. Without a detailed calculation of the infall process, however, it is difficult to judge whether our neglect of infall is really satisfied or whether a more realistic model calculation should include such source terms.

The differential equation (18) describes the time evolution in a comoving frame for each species i in the gas phase within a specific parcel of matter. We have one such equation for each species i. This system of ordinary differential equations has to be solved together with the equations (3), (4) and (6) for the disk structure and an equation for the opacity. Since

- the opacity changes due to formation or destruction of absorbers by chemical reactions and since
- the temperature in the disk changes if the opacity changes and since
- the rates of the chemical processes change if the temperature changes which in turn strongly influences the further chemical evolution of the system,

the structure of the disk and the chemistry in the disk are closely coupled. For this reason the differential equations for the chemical evolution and the equations for the disk structure need to be solved simultaneously. They form a system of *Differential Algebraic Equations* which requires special methods for its solution. The method used in our calculation for the solution of such systems is described in detail Paper I.

3.3. The chemical reaction network

In Paper I we modeled the chemistry of the four most abundant elements H, C, N and O. In this work we add the silicon and the sulfur chemistry to our chemical network. The silicon chemistry is initiated by the evaporation of the olivine dust particles, which mainly injects SiO into the gas phase. This SiO then undergoes a lot of gas phase reactions which results in the formation of some other abundant silicon bearing molecular species. The sulfur chemistry becomes active at elevated temperatures, when the troilite particles (FeS) start to evaporate (see Sect. 4.1 for a description of our dust model) which mainly injects Fe and S atoms into the gas phase. The S then undergoes a lot of gas phase reactions to form other abundant sulfur bearing molecules especially H_2S.

For the neutral-neutral reactions of the HCON chemistry we use the gas phase reactions given by Mitchell (1984)[2]. The system of Mitchell is extended and updated by some reactions given in Baulch et al. (1992). In the list of Baulch et al. the equilibrium constants of most of the reactions are included. Some backward reactions could then be calculated and added to the system. The reactions for the sulfur chemistry and some reactions for the silicon chemistry are taken from Millar et al. (1991)[3]. The sili-

[2] Corrected for some misprints in that list.

[3] We used the updated version of the list of reaction rates obtained from the WWW

con chemistry has been completed with the gas phase reactions given in Britten et al. (1990).

In the present work we treat a system of totally 106 molecular and atomic species (i.e. 106 differential equations) coupled by about 600 chemical reactions. The system is complemented by three differential equations for the radius changes of the three different dust components (carbon, olivine and troilite – see Sect. 4.1).

A few ternary reactions are included in our chemical reaction network

$$H_2 + H + H \longleftrightarrow H_2 + H_2 \quad (20)$$

$$H + H + H \longleftrightarrow H + H_2\,, \quad (21)$$

which lead to the formation of H_2. The first reaction is surprisingly active in the outer parts of the disk, where the density of H_2 is high. The second is important in the innermost parts of the disks and counteracts for a while the molecular hydrogen dissociation (at ≈0.1 AU). The rate coefficients of these reactions are taken from Baulch et al. (1992).

Olivine and troilite particles inject during their thermal decomposition SiO and O (for olivine) and S (for troilite) into the gas phase and additionally corresponding amounts of magnesium and iron atoms. The Mg and Fe atoms are not involved in in our reaction network for the neutral chemistry and remain simply as free atoms in the gas phase.

4. Model assumptions

4.1. The dust model

We assume that three dust components are present in the disk matter: olivine, carbon dust and troilite. For a more complete description of our dust model, we refer to Paper II. The main features of our dust and ice model including the new assumptions concerning troilite are the following:

Ices We suppose, that different sorts of ices are frozen out on the grains surface at large distances from the protostar (>25 AU). H_2O and CO are the most abundant species but small amounts of CH_3OH, NH_3, and some other species are present, too (Pollack et al. 1994). We will neglect the species with low abundances and assume that only the two dominating components water and carbon monoxide form coatings on the grains. We have separated the H_2O and the CO ice in two distinct layers. CO should be the outer one because it has the lowest vapourisation temperature (≈30 K, e.g. Sandford and Allamandola 1993). H_2O vapourises at higher temperatures (≈150 K) and forms the inner layer. This model is of course too simple: CO and water ice can be mixed and CO molecules are able even at rather low temperatures to diffuse through the H_2O matrix and/ or they are trapped in a clathrate structure within the water ice (Sandford and Allamandola 1988, 1990a, 1990b, 1993, Lunine and Stephenson 1985), depending on the lattice position. Laboratory experiments show that CO and other volatiles are released at several distinct temperatures (e.g. Hudson and Donn 1991). Part of the CO is released not until the water ice starts to evaporate at about 150 K. We neglect such complications in this paper and simply treat H_2O and CO as two separate ice components. The corresponding rate terms for H_2O and CO evaporation and recombination with the surface, respectively, are added to the continuity equation (16) for H_2O and CO.

Carbon dust The carbon dust is simply assumed to be graphite, as in Paper I and II, though this certainly is an oversimplification. The exact nature of interstellar carbon grains is unclear. The carbon found in meteorites (the kerogenes) is a chemically processed material which probably formed in the solar nebula (Cronin et al. 1988) though an at least partial extra solar nebular origin of the carbon material found in meteorites cannot be excluded (Wright and Gilmour 1990)[4].

For carbon dust we use the thermodynamical properties of graphite as in Paper II. According to the assumed MRN distribution for the grains (see below), 70% of the available carbon is bound in graphite. The remaining fraction is supposed to be present as CO.

Silicate dust According to the results of Mathis et al. (1977), silicon bearing dust of the form $Mg_xFe_{2-x}SiO_4$ is present in the interstellar medium. The value of x is unclear. We will then suppose that x = 2, i.e., no iron is present in this dust. We take Mg_2SiO_4 as model for the silicon dust. The omission of iron atoms in the dust is not important since iron doesn't participate in the chemistry in our reaction network. Furthermore the thermodynamical properties of olivine (Mg_2SiO_4) are known and thus we can calculate the vapour pressure (Duschl et al 1996).

Troilite The iron sulfide FeS (Troilite) has been added to the calculation as an additional dust component. It is known, that troilite particles are present in meteorites and, thus, in the early solar system. It seems likely that they are already present in the parent molecular cloud and that they constitute a major sulfur bearing material. For details see the discussion in Pollack et al. (1994). They propose the following model for the abundance of S bearing species: the abundance of FeS in the disk corresponds to 75% of the solar system abundance of S, about 20% of S should be present as S or H_2S in the gas phase and 5% as part of the ice coatings (H_2S, SO, SO_2). They argue that a certain fraction of the iron contained in the molecular cloud dust is converted into FeS during the passage of the accretion shock and that the abundance of FeS in the molecular cloud material corresponds to roughly 50% of the sulfur abundance. Since at present there is no definite hint that part of the Fe is really converted to FeS in passing the accretion shock, we prefer to assume that one half of the available sulfur *in the disk* is bound in these troilite particles.

[4] We do not consider the tiny fraction of isotopic peculiar dust which is unprocesses circumstellar dust material from dying stars

4.2. Destruction of silicate dust

Silicate dust is destroyed by thermal decomposition above ≈1 650 K according to the same process as described in detail in Paper II

$$Mg_2SiO_4\,(\text{solid}) \longrightarrow 2Mg + SiO + 3O\,. \quad (22)$$

In the calculation presented in Paper I, the SiO does not undergo further chemical reactions, until collisional dissociation becomes possible. The newly added gas phase silicon chemistry leads to supplementary silicon bearing species. The different pathways of the silicon chemistry are explained in Sect. 5.2.

The dust can partially or completely be destroyed in passing the accretion shock for infall velocities $\gtrsim 100\,\mathrm{km\cdot s^{-1}}$ (Shull 1977, Draine and Salpeter 1979) and in this case is later reformed somewhere behind the shock. We consider in this paper a late phase of the star formation process where most of the mass is already concentrated in the star and the remaining infall of matter occurs at large distances (Cassen 1994) where the accretion shock is likely to be too weak to destroy the dust particles. Only the ice coatings first vapourise and later re-condense in passing the shock (Lunine et al. 1991). Thus, we simply assume that the dust equals the unmodified interstellar dust. We, then, assume the standard MRN (Mathis et al. 1977) size distribution for the ensemble of dust particles including the ice layers

$$f(a)\,da = Ca^{-\frac{7}{2}}da\,. \quad (23)$$

a is the particle radius and C is a constant ($\log C = -15.14$ for silicate dust and $\log C = -15.20$ for carbon dust). The method for calculating the decomposition of an ensemble of grains with such a size distribution is described in Paper II.

The rate terms corresponding to the different destruction, evaporation, and re-condensation processes are added as source terms to the continuity equation (16) for the corresponding species.

4.3. Oxidation of the carbon dust

Carbon dust can be destroyed by different mechanisms. In Paper I we treated carbon destruction by pure evaporation. The evaporation starts to be effective at a temperature of ≈1 500 K and C_i molecules (mainly i=1, 2, 3) are injected into the gas phase. These molecules undergo a lot of gas phase reactions until they are finally converted into CO (see Paper I for a detailed description of the pathways). There exist two additional possibilities for carbon destruction: chemical sputtering with H atoms and oxidation by O atoms or oxygen bearing molecules. Sputtering by H is discussed in Lenzuni et al. 1995. We believe this process to be not important for the protoplanetary disk (see Paper II) but this process may be important in hot molecular cores or for the material directly entering the protostar in the early collapse phase. In this paper we consider the oxidation process.

Different oxygen bearing species are able to react with C atoms on the surface of the carbon grains. From flame chemistry under laboratory conditions it is known that the most significant molecules for the oxidation of graphite are OH and O_2 (El–Gamal 1995). Under the conditions encountered in the protoplanetary accretion disk the molecular oxygen has a much too low abundance as to be important (any O_2 would be rapidly converted to H_2O in reactions with H and H_2 in the hydrogen rich environment). However, OH becomes moderately abundant at elevated temperatures when H_2 starts to dissociate and the H atom reacts with H_2O

$$H + H_2O \longrightarrow OH + H_2 \quad (24)$$

to form OH.

The essential first reaction step in the oxidation of soot (carbon dust) by OH radicals is (El–Gamal 1995)

$$\text{soot}_{N+2} + OH \longrightarrow \text{soot}_N + HCCO\,. \quad (25)$$

The reaction has a measured probability of 0.1 . . . 0.2 to occur during a collision (Neoh et al. 1981, 1984, Garo et al. 1990, Roth et al. 1990, 1992). This key reaction cracks a six-ring at the periphery of the huge PAH's forming the carbon dust particles and transfers two carbon atoms into the gas phase:

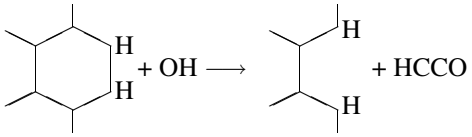

The ketyl radical HCCO reacts then in the gas phase with H as follows

$$HCCO + H \longrightarrow CO + CH_2\,. \quad (26)$$

One of the carbon atoms is immediately converted by this reaction into CO and the other one forms a methylene radical CH_2. The CH_2 radical resulting from this reaction then reacts with the molecular hydrogen to form a methyl radical, that in turn reacts with H_2 to form ultimately methane

$$CH_2 \overset{+H_2}{\longleftrightarrow} CH_3 \overset{+H_2}{\longrightarrow} CH_4\,. \quad (27)$$

As we shall see in Sect. 5, this process is of considerable significance for the chemical composition of the disk matter.

This process of carbon grain destruction starts to operate in an accretion disk already at a temperature of about 1 000 K.

Also, the reaction with free oxygen atoms has a significant reaction probability (Roth et al. 1990, von Gersum S. and Roth P.1992). The oxidation process of graphite particles by free O atoms is (Warnatz, personal communication)

$$\text{soot}_{N+1} + O \longrightarrow \text{soot}_N + CO\,. \quad (28)$$

In this case the liberated C atom is promptly locked in CO and is lost for the hydrocarbon chemistry. We have included this process in the calculation but it becomes never important in the protoplanetary disk because the only source of noticeable amounts of free O atoms is the decomposition of the silicates particles which starts at about 1 650 K. At this temperature the carbon dust has already disappeared because of erosion by OH.

4.4. Vapourisation of troilite particles

FeS particles in a hydrogen rich environment start at a temperature of $\approx$ 690 K to be reduced to pure iron particles according to the reaction

$$\mathrm{FeS\,(solid)\ +\ H_2\ \longrightarrow\ Fe\,(solid)\ +\ H_2S}$$

(e.g. Fegley and Prinn 1989). On the other hand, at a temperature slightly above $\approx$700 K the FeS particles start to vapourise and they inject in this case mainly free sulfur and iron atoms into the gas phase. It can be shown from thermodynamical calculations that small amounts of FeS molecules are present in the vapour, too, but their abundance in the gas phase is about a factor of 10 lower than the Fe and S abundances. So we will neglect them. The vapourisation process of troilite is therefore assumed to be

$$\mathrm{FeS\,(solid)\ \longrightarrow\ Fe\ +\ S\,.}$$

The sulfur atoms in the gas phase are rapidly converted into H_2S. Since both processes, vapourisation and reduction to Fe, occur at approximately the same temperature we neglected in this calculation the process of conversion of FeS into Fe particles in order to avoid to solve an additional equation for iron particles. The result for the gas phase sulfur chemistry is identical for all practical purposes.

The equilibrium vapour pressures p_{Fe} and p_{S} of Fe and S, respectively, over solid FeS satisfy

$$1 = p_{\mathrm{Fe}} p_{\mathrm{S}} \exp(-\frac{\Delta G}{RT}) \tag{29}$$

according to the law of mass action. If only Fe and S atoms are injected into the gas phase, we have $p_{\mathrm{Fe}} = p_{\mathrm{S}}$ and then

$$p_{\mathrm{Fe}} = p_{\mathrm{S}} = \exp(\frac{\Delta G}{2RT})\,. \tag{30}$$

ΔG is the free enthalpy of formation of the troilite particles from their constituents in the gas phase. We calculate ΔG for troilite from the polynomial fit given in Sharp and Huebner (1990).

The radius change of a given grain is

$$\frac{\mathrm{d}a}{\mathrm{d}t} = -\alpha_{\mathrm{FeS}} V_0 \frac{p_{\mathrm{S}}}{kT} v_{\mathrm{FeS}} \tag{31}$$

and the variation in the particle densities of S and Fe is

$$\frac{\mathrm{d}n_{\mathrm{S}}}{\mathrm{d}t} = \frac{\mathrm{d}n_{\mathrm{Fe}}}{\mathrm{d}t} = 4\pi a^2 \alpha_{\mathrm{FeS}} v_{\mathrm{FeS}} \frac{p_{\mathrm{S}}}{kT}\,. \tag{32}$$

v_{FeS} is the thermal velocity of the FeS molecules, V_0 is the volume occupied by the nominal molecule in the condensate and α_{FeS} is the so called sticking coefficient which is assumed to be α_{FeS}=0.1.

For troilite grains we assume that they all have the same initial radius since they don't provide an essential contribution to the total opacity and, thus, do not significantly modify the disk structure due to their opacity. Usually, for a major dust component the finite width of the size distribution has to be considered in order to avoid that all the grains disappear instantaneously. A test calculation has shown that this causes a discontinuous slope of the opacity which leads to serious numerical difficulties for high order solution schemes for ODE's, like that used in our calculation.

Table 2. Solar system element abundances (Anders and Grevesse 1989, Grevesse and Noels 1993)

Z	Element		$\log \epsilon_{And}$	ϵ/ϵ_H
1	Hydrogen	H	12.00	1.00
2	Helium	He	10.99	$9.75 \cdot 10^{-2}$
6	Carbon	C	8.55	$3.55 \cdot 10^{-4}$
7	Nitrogen	N	7.97	$9.33 \cdot 10^{-5}$
8	Oxygen	O	8.93	$7.41 \cdot 10^{-4}$
12	Magnesium	Mg	7.59	$3.85 \cdot 10^{-5}$
14	Silicon	Si	7.55	$3.58 \cdot 10^{-5}$
16	Sulfur	S	7.27	$1.85 \cdot 10^{-5}$
26	Iron	Fe	7.51	$3.24 \cdot 10^{-5}$

4.5. Initial conditions

The chemical composition of the material at the outer disk's edge should not be very different from the composition of the parent molecular cloud. The abundances ϵ_{X} used in the calculation are solar system abundances as given by Anders and Grevesse (1989) and Grevesse and Noels (1993) (c.f. Tab 2). If we define $N_{\mathrm{H}} = 2n_{\mathrm{H_2}} + n_{\mathrm{H}}$ (total amount of hydrogen nuclei), we set initially

$$n_{\mathrm{H}} = 10^{-5}\, N_{\mathrm{H}}\,,$$

the remaining fraction being mostly H_2. This assumption is somewhat arbitrary. It has been chosen to allow a rapid settling of chemical equilibrium between H_2 and H.

Helium and nitrogen are assumed to enter the accretion disk as He atoms and N_2 molecules. These two gases have very low condensation temperatures and are assumed not to be condensed onto grains (e.g. Yamamoto 1985). Their abundances in the gas phase are

$$n_{\mathrm{He}} = \epsilon_{\mathrm{He}}\, N_{\mathrm{H}}\,. \tag{33}$$

and

$$n_{\mathrm{N_2}} = \frac{1}{2}\epsilon_{\mathrm{N}}\, N_{\mathrm{H}} \tag{34}$$

The small amounts of NH_3, NO, and HCN observed to be present in star forming regions (van Dishoeck et al. 1993) are neglected in this calculation.

Since 70% of the carbon atoms are bound in carbon dust and since the remaining fraction is bound in CO, we have

$$n_{\mathrm{CO}} = 0.3\,\epsilon_{\mathrm{C}}\, N_{\mathrm{H}}\,. \tag{35}$$

This CO is assumed to be frozen onto the surface of the dust grains. A small fraction of the carbon is bound in less abundant molecules, for instance CH_4, CH_3OH, H_2CO, HCN, CS (van Dishoeck et al. 1993). Most of them will initially be condensed in the ice mantles. We neglect them in the present model calculation.

The fraction of oxygen that is not bound in CO or in silicate grains is supposed to be present as water ice. We have in this case

$$n_{H_2O} = (\epsilon_O - 0.3\epsilon_C - 4\epsilon_{Si})\, N_H\,. \quad (36)$$

The thicknesses of the resulting ice layers are calculated from n_{CO} and n_{H_2O} as described in Paper I.

The assumption that all the remaining oxygen is present as water ice is somewhat doubtful because in molecular clouds the available oxygen never is completely bound in water molecules but is partially bound in O or O_2. However, the accretion shock at the disk edge modifies the chemical composition of the infalling material. The material from the surrounding cloud "falls" onto the disk with velocities ranging from 10 km s^{-1} at $s \approx 10$ AU to 100 km s^{-1} at $s \approx 1$ AU (Cassen 1994). Immediately behind the shock the temperature can raise up to several 1 000 K (Neufeld and Hollenbach 1994) and our calculations show that most of the neutral-neutral chemistry becomes active at about such temperatures. The model of Neufeld and Hollenbach (1994) has shown that any atomic or molecular oxygen efficiently is converted into water molecules which later will freeze out on the surface of the grains (Lunine et al. 1991).

The available sulfur is assumed to be partially bound into FeS grains (50%). The remaining fraction stays in the gas phase. In the parent molecular cloud much of the sulfur will be bound into SO, SO_2 or is present as the free S atom and some of the gases may be frozen onto grains. As in the case of oxygen, it is to be expected that ice mantles evaporate in passing the accretion shock and that most of the sulfur contained in the gas phase is converted into H_2S. The H_2S has a rather low condensation temperature (cf. Yamamoto 1985 or Sandford and Allamandola 1993). For simplicity we assume that the H_2S remains completely in the gas phase and choose

$$n_{H_2S} = 0.5\,\epsilon_S\, N_H\,. \quad (37)$$

We prescribe the above defined chemical composition of the gas parcel at the outer edge of the accretion disk. We have chosen an outer disk radius of 40 AU since this is approximately the size of most of the observed disks (Ruden and Pollack 1991) and of our solar system. This parcel moves inwards with the velocity (5) and our model calculation follows the gas parcel and calculates its chemical composition at each distance s.

5. Results and interpretation

Fig. 3 shows the chemical composition of the gas phase in the disk's central plane between 7.3 and 0.13 AU. The CO ice already vapourises at ≈21 AU ($T \approx$30 K) and the water ice at ≈8 AU ($T \approx$150 K). At 7.3 AU all the volatile species are in the gas phase. The density of free H atoms is well under the initial concentration of $10^{-5}\, N_H$ because of H_2 formation by three body collisions (20). At this distance from the protostar the gas phase is composed only of H_2, H, N_2, CO, H_2O, some H_2S, and He and this composition prevails until the temperatures required for the onset of dust destruction are reached.

5.1. Oxidation of the carbon dust

The carbon dust oxidation has dramatic effects on the chemical composition of the gas phase. As a direct consequence of the oxidation process (25) and the follow up reactions (26) and (27), we observe a huge amount of methane as temporary product between 1.5 and 0.8 AU ($T \approx$1 000 and 1 200 K) i.e. *in the actual vicinity of the Earth*. In our previous work (Paper I) we have also observed a maximum for the methane abundance approximately in the same region of the disk but the density of methane was of about a factor 10^4 lower. We discuss the processes responsible for methane formation and its conversion to CO in some detail.

5.1.1. Methane formation

When the carbon dust is attacked by OH radicals in the first step (25) the ketyl radical HCOO is formed which immediately reacts according to HCCO + H $\longrightarrow$ CO + CH_2 (Eq. 26). This forms (i) a CO molecule which does not further participate in the chemistry of the gas phase due its high bond energy and (ii) a CH_2 radical which reacts rapidly with the abundant H_2 to produce methane according to the reaction chain

$$\begin{aligned} CH_3 + H_2 &\underset{k_{-4}}{\overset{k_4}{\rightleftharpoons}} CH_4 + H \quad (38)\\ CH_2 + H_2 &\underset{k_{-3}}{\overset{k_3}{\rightleftharpoons}} CH_3 + H\\ CH + H_2 &\underset{k_{-2}}{\overset{k_2}{\rightleftharpoons}} CH_2 + H\\ C + H_2 &\underset{k_{-1}}{\overset{k_1}{\rightleftharpoons}} CH + H\,. \end{aligned}$$

These reactions are energetically nearly neutral and involve no substantial activation energy barriers. We have calculated typical reaction timescales at a typical pressure of 100 dyn·cm^{-2} (cf. Eq. (4)) and temperatures between 1 000 K and 1 500 K (c.f. Eq. (3)) using rate coefficients from Mitchell (1984) and assuming chemical equilibrium abundances of H atoms. The results are shown in Table 3.

An inspection of Table 3 shows that reaction timescales range between 10^4 s and 1 s for the hydrogen abstraction reactions with H and between 1 s and 10^{-2} s for the hydrogen addition reactions with H_2. These timescales are short compared to the characteristic timescale for changes of pressure and temperature $\tau_{hyd} = s/v_s \approx 10^{12}$ s. Thus, there quickly establishes an equilibrium where the CH_2 initially injected into the gas phase is distributed over the compounds C, CH, CH_2, CH_3 and CH_4. Most of the carbon remains as CH_4 in the gas phase since hydrogen addition reactions occur much more frequently than hydrogen abstraction reactions due to the high abundance of molecular H_2. Only if the temperature has climbed to ≈ 1500K, a substantial fraction of the carbon would be converted into CH_3 because then there is a considerable abundance of free hydrogen atoms. Since the reactions with hydrogen are so rapid, any reaction involving one of the considerably less abundant heavier elements cannot significantly disturb this equilibrium state between the CH_n compounds and we can safely assume that the

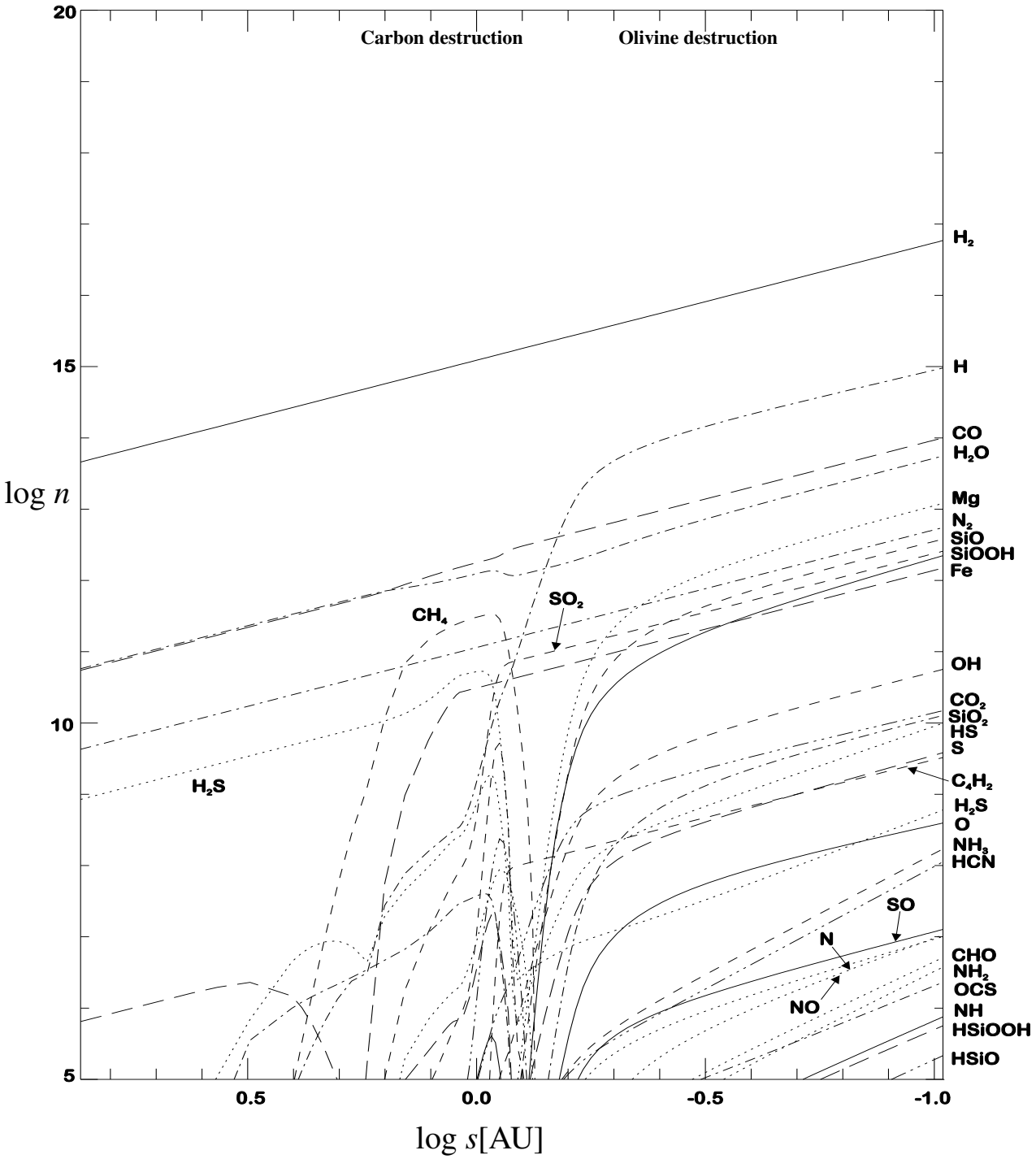

Fig. 3. Run of molecular abundances in the accretion disk in the region of dust destruction.

abundance of these molecules always equals their abundance according to a stationary state between the reactions (38)

$$\begin{aligned} \frac{n_{\rm CH}}{n_{\rm C}} &= \frac{k_1}{k_{-1}}\frac{n_{\rm H_2}}{n_{\rm H}} \\ \frac{n_{\rm CH_2}}{n_{\rm CH}} &= \frac{k_2}{k_{-2}}\frac{n_{\rm H_2}}{n_{\rm H}} \end{aligned} \tag{39}$$

$$\begin{aligned} \frac{n_{\rm CH_3}}{n_{\rm CH_2}} &= \frac{k_3}{k_{-3}}\frac{n_{\rm H_2}}{n_{\rm H}} \\ \frac{n_{\rm CH_4}}{n_{\rm CH_3}} &= \frac{k_4}{k_{-4}}\frac{n_{\rm H_2}}{n_{\rm H}} . \end{aligned}$$

Table 3 shows the abundances of CH_n ($n = 0, \ldots, 3$) relative to CH_4 in kinetical equilibrium with H and H_2. Since we assumed dissociation equilibrium for hydrogen in the gas phase, these

Table 3. Relative abundance of CH_n molecules in kinetic equilibrium and timescales (in sec) for reactions with H and H_2 at a pressure of 100 dyn cm^{-2} at different temperatures

	1000 K	1200 K	1500 K
n_{CH_3}/n_{CH_4}	$1.85\,10^{-5}$	$1.91\,10^{-3}$	$2.05\,10^{-1}$
$\tau_{CH_3\rightarrow CH_4}$	$2.90\,10^{-1}$	$1.39\,10^{-1}$	$6.97\,10^{-2}$
$\tau_{CH_4\rightarrow CH_3}$	$1.57\,10^{+4}$	$7.25\,10^{+1}$	$3.41\,10^{-1}$
n_{CH_2}/n_{CH_4}	$1.03\,10^{-11}$	$8.10\,10^{-8}$	$6.75\,10^{-4}$
$\tau_{CH_2\rightarrow CH_3}$	$1.54\,10^{-2}$	$6.18\,10^{-3}$	$2.56\,10^{-3}$
$\tau_{CH_3\rightarrow CH_2}$	$2.78\,10^{+4}$	$1.46\,10^{+2}$	$7.77\,10^{-1}$
n_{CH}/n_{CH_4}	$4.54\,10^{-20}$	$6.11\,10^{-14}$	$8.90\,10^{-8}$
$\tau_{CH\rightarrow CH_2}$	$2.19\,10^{-1}$	$5.36\,10^{-2}$	$1.33\,10^{-2}$
$\tau_{CH_2\rightarrow CH}$	$4.95\,10^{+7}$	$7.11\,10^{+4}$	$1.01\,10^{+2}$
n_C/n_{CH_4}	$6.18\,10^{-22}$	$9.93\,10^{-15}$	$1.78\,10^{-7}$
$\tau_{C\rightarrow CH}$	$2.58\,10^{+1}$	$2.69\,10^{+0}$	$2.88\,10^{-1}$
$\tau_{CH\rightarrow C}$	$1.90\,10^{+3}$	$1.66\,10^{+1}$	$1.44\,10^{-1}$

abundance ratios are as in chemical equilibrium. Even if the hydrogen dissociation is far from a chemical equlibrium state the reaction timescales are so short compared to the hydrodynamic timescale that their density ratios always equal their stationary equlibrium ratios given by (39).

The CH_n molecules form the starting point for further reactions which may lead finally to CO.

5.1.2. Reactions with oxygen bearing compounds

The most abundant oxygen bearing compounds prior to dust destruction are H_2O and CO (cf. Fig. 3). Reactions with the CO molecule are energetically forbidden by the high bond energy of the CO molecule. Reactions with H_2O, however, are possible.

The CH_n for $n = 0, \ldots, 3$ exchange a hydrogen atom in reactions with the water molecule:

$$CH_n + H_2O \underset{k_{-5}}{\overset{k_5}{\rightleftarrows}} CH_{n+1} + OH\,. \tag{40}$$

These reactions are rapid, but they cannot compete with the rapid reactions (38) and do not significantly modify the equilibrium between the CH_n. Reactions between water and the CH_n, in which an OH group would be attached to the carbon atom are slightly endothermic (≈ 1 eV) and cannot occur. Reactions between H_2O and CH_n in which the formaldehyde molecule H_2CO or the formyl radical HCO are formed are strongly exothermic but seem not to occur, probably since the alternative reaction (40) is easier.

The next abundant oxygen bearing molecule is OH, which is formed by the reaction

$$H_2O + H \longleftrightarrow OH + H_2$$

at the onset of hydrogen dissociation. The OH easely reacts with hydrocarbons by the reactions (40), but this does not form a bond between C and O. Possible reactions which do form a C-O-bond result in formaldehyde

$$CH_2 + OH \xrightarrow{k_6} H_2CO + H \tag{41}$$

or formyl

$$CH + OH \xrightarrow{k_7} HCO + H\,. \tag{42}$$

The reverse of reactions (41) and (42) are endothermic by 69.3 and 90.3 kcal/ mol, respectively, and thus are energetically forbidden. The resulting formaldehyde is readily transformed into formyl by the hydrogen abstraction reaction

$$H_2CO + H \underset{k_{-8}}{\overset{k_8}{\rightleftarrows}} HCO + H_2 \tag{43}$$

and the formyl is readily transformed into CO by

$$HCO + H \xrightarrow{k_9} CO + H_2\,. \tag{44}$$

These reactions are rapid. The reverse of reaction (44) is forbidden since it is endothermic by $\Delta H = -87.5$ kcal/ mol and forms a one way to CO. Characteristic timescales for these reactions have been computed with the rate coefficients given by Mitchell (1984) with the assumption that dissociation of H_2 and H_2O is as in chemical equilibrium. The results are shown in Table 4. An inspection of this table shows that only reaction (41) is a possible pathway to convert the CH_n molecules by reactions

Table 4. Reaction timescales for reactions important for the conversion of hydrocarbons to CO at a pressure of 100 dyn cm^{-2} at different temperatures. This is the average time required for the first molecule to react with the second one

	1000 K	1200 K	1500 K
$\tau_{H_2CO+H\rightarrow HCO+H_2}$	$3.61\,10^{+3}$	$1.68\,10^{-1}$	$1.38\,10^{-1}$
$\tau_{HCO+H_2\rightarrow H_2CO+H}$	$3.48\,10^{+2}$	$2.57\,10^{+1}$	$1.91\,10^{+0}$
$\tau_{HCO+H\rightarrow CO+H_2}$	$2.21\,10^{+1}$	$3.06\,10^{-1}$	$4.29\,10^{-3}$
$\tau_{CH_2+OH\rightarrow H_2CO+H}$	$3.61\,10^{+9}$	$9.02\,10^{+6}$	$2.34\,10^{+4}$
$\tau_{CH+OH\rightarrow HCO+H}$	$2.80\,10^{+10}$	$4.22\,10^{+7}$	$6.48\,10^{+4}$
$\tau_{CH_3+O\rightarrow H_2CO+H}$	$1.96\,10^{+14}$	$1.01\,10^{+10}$	$5.30\,10^{+5}$
$\tau_{CH_2+O\rightarrow HCO+H}$	$4.59\,10^{+15}$	$1.55\,10^{+11}$	$5.19\,10^{+6}$
$\tau_{CH_2+O\rightarrow CO+H+H}$	$1.96\,10^{+14}$	$1.01\,10^{+10}$	$5.30\,10^{+5}$
$\tau_{CH_3+CH_3\rightarrow C_2H_5+H}$	$1.63\,10^{+7}$	$4.23\,10^{+4}$	$1.11\,10^{+2}$
$\tau_{C_2H_5+H\rightarrow 2CH_3}$	$1.31\,10^{+1}$	$9.50\,10^{-2}$	$6.87\,10^{-4}$
$\tau_{CH_3+CH_3\rightarrow C_2H_4+H_2}$	$3.25\,10^{+10}$	$1.03\,10^{+7}$	$3.30\,10^{+3}$
$\tau_{CH_3+CH_2\rightarrow C_2H_4+H}$	$3.54\,10^{+10}$	$5.54\,10^{+6}$	$8.32\,10^{+2}$
$\tau_{C_2H_4+H\rightarrow C_2H_3+H_2}$	$4.57\,10^{+3}$	$2.67\,10^{+1}$	$4.28\,10^{+0}$
$\tau_{C_2H_3+H_2\rightarrow C_2H_4+H}$	$5.90\,10^{-3}$	$4.36\,10^{-3}$	$3.34\,10^{-3}$
$\tau_{C_2H_3+H\rightarrow C_2H_2+H_2}$	$4.44\,10^{+2}$	$6.12\,10^{+0}$	$8.59\,10^{-2}$
$\tau_{C_2H_2+H\rightarrow C_2H+H_2}$	$2.68\,10^{+5}$	$7.83\,10^{+2}$	$2.33\,10^{+0}$
$\tau_{C_2H+H_2\rightarrow C_2H_2+H}$	$3.82\,10^{-4}$	$1.36\,10^{-4}$	$3.56\,10^{-4}$
$\tau_{C_2H_4+O\rightarrow HCO+CH_3}$	$2.22\,10^{+15}$	$5.43\,10^{+10}$	$3.25\,10^{+6}$
$\tau_{C_2H+O\rightarrow CH+CO}$	$9.59\,10^{+14}$	$3.11\,10^{+10}$	$2.59\,10^{+6}$

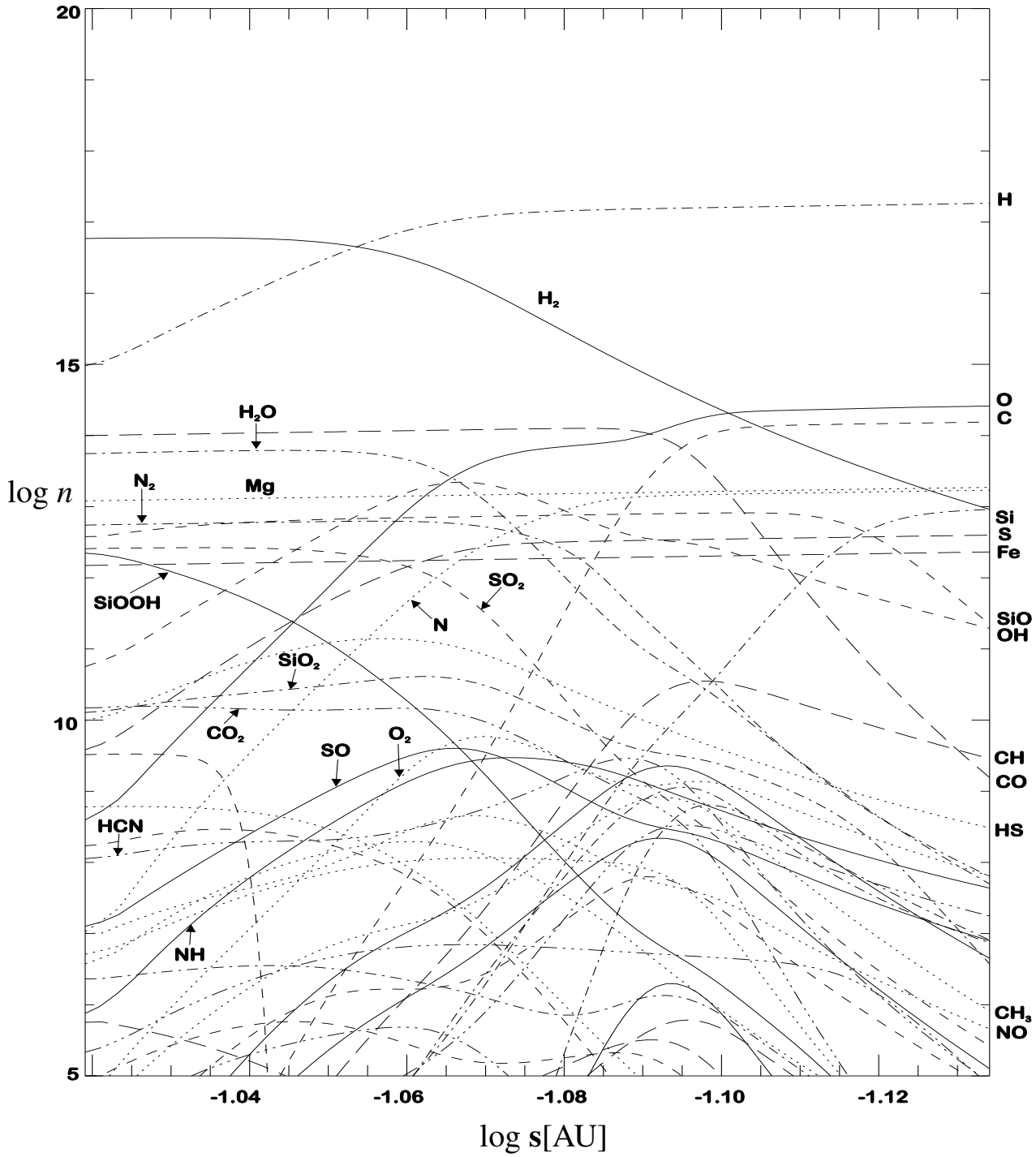

Fig. 4. Run of molecular abundances in the accretion disk in the innermost region of molecule dissociation.

wit OH into CO. The abundance of CH is much too low for the reaction (42) to compete with (41), except for the highest temperature.

Finally we have to consider reactions with free oxygen atoms. One possible type of reaction with CH_n is

$$CH_n + O \rightleftharpoons CH_{n-1} + OH\,.$$

Such reactions are fast, but they do not lead to CO formation and they cannot compete with the much more frequent reactions (40), i.e., they are unimportant. Possible reactions leading to formation of a C-O-bond are

$$CH_2 + O \xrightarrow{k_{10}} CO + H + H \quad (45)$$

$$CH_2 + O \xrightarrow{k_{11}} HCO + H \quad (46)$$

$$CH_3 + O \xrightarrow{k_{12}} H_2CO + H\,. \quad (47)$$

These reactions are strongly exothermic and only occur in the indicated direction. Calculated timescales for these reactions using data from Mitchell (1984) are given in Table 4. Since the abundance of O is quite small, the timescales are rather long for low temperatures and only become short at a temperature of ≈ 1500 K due to the increasing degree of dissociation of water molecules. In any case, the reactions (42) and (45), ..., (47) cannot compete with the much more frequent reaction (41) and are unimportant for the CO formation.

We conclude that the dominant *direct* pathway from sputtering products of carbon dust to CO is the reaction chain (41), (43), and (44). Inspection of Table 4 shows that the rate determining step is reaction (41). Every CH_2 reacting with OH rapidly reacts further to CO. However, since the reaction from the products CH_n of carbon sputtering to CO requires a reaction path involving the rare molecules CH_2 and OH, the reaction to CO is slow and the CH_4 and the unsaturated CH_n molecules accumulate in the gas phase until their abundance has raised to a level where subsequent reactions to CO operate with a rate comparable to the sputtering rate. In this case, a high abundance of CH_n molecules develops in the gas phase. This can clearly be seen from Fig. 3. A reaction between the saturated CH_4 molecules is not possible, but if the radicals $CH_i (i = 0, \ldots, 3)$ have formed in sufficient amounts then reactions between such radicals become important. As a consequence of this, there exists a more efficient indirect pathway to CO formation.

5.1.3. The pathway to acetylene

Reactions, in which a hydrogen atom is exchanged between CH_n and CH_m are rapid, but they do not significantly modify the equilibrium between these hydrocarbons and hydrogen and, thus, can be neglected. However, there exist some condensation reactions which form higher hydrocarbons:

$$CH_3 + CH_3 \underset{k_{-13}}{\overset{k_{13}}{\rightleftharpoons}} C_2H_5 + H \quad (48)$$

$$CH_3 + CH_3 \xrightarrow{k_{14}} C_2H_4 + H_2 \quad (49)$$

$$CH_2 + CH_3 \xrightarrow{k_{15}} C_2H_4 + H \quad (50)$$

The formation of C_2H_5 is slightly endothermic ($\Delta H \approx 10$ kcal/ mol) and occurs preferentially from the right to the left. If we arbitrarily assume that 10% of the carbon grain material is present in the gas phase as CH_4 we can calculate the reaction timescales. We use the rate coefficient for the forward reaction as given by Mitchell (1984) and calculate that for the reverse direction from a Milne relation. Results for the timescales are given in Table 4. We can see that every C_2H_5 molecule formed in the forward reaction (48) is immediately destroyed by the backwards reaction. Thus, any further reaction path starting at C_2H_5 will be inefficient and we do not consider this case further.

The reactions (49) and (50) are strongly exothermic and occur only in the direction of formation of a C-C-bond. Calculated timescales are given in Table 4. These reactions convert some of the CH_3 to ethylene C_2H_4. The ethylene will be subject to the following sequence of reactions with hydrogen

$$C_2H_4 + H \underset{k_{-16}}{\overset{k_{16}}{\rightleftharpoons}} C_2H_3 + H_2 \quad (51)$$

$$C_2H_3 + H \xrightarrow{k_{17}} C_2H_2 + H_2 \quad (52)$$

$$C_2H_2 + H \underset{k_{-18}}{\overset{k_{18}}{\rightleftharpoons}} C_2H + H_2 \quad (53)$$

Reactions (51) and (53) are mildly exothermic ($\Delta H \approx 4.4$ and 15.5 kcal/ mol, respectively) and preferentially occur in the backwards direction. Reaction (52) is exothermic by $\Delta H \approx -66.9$ kcal/ mol and acts only in the direction of acetylene formation. Reaction timescales using rate coefficients given by Frenklach and Feigelson (1989) are given in Table 4. The reactions (51) and (53) are rapid and each establishes an equilibrium between C_2H_4 and C_2H_3 or between C_2H_2 and C_2H, respectively. Most of the carbon will be in ethylene and acetylene. Additionally, reactions with OH are possible in which a hydrogen is exchanged but these cannot compete with the more frequent reactions with H.

5.1.4. The pathway to CO

Reactions with O to form a C-O-bond are possible for C_2H_4 and C_2H

$$C_2H_4 + O \xrightarrow{k_{19}} HCO + CH_3 \quad (54)$$

$$C_2H + O \xrightarrow{k_{20}} CH + CO\,. \quad (55)$$

The acetylene is known from flame chemistry only to form OH in reactions with O but not to close a C-O-bond. Calculated timescales for these reactions using rate coefficients from Baulch et. al. (1992) are given in Table 4. These reactions are inefficient unless the temperature has increased sufficiently and free oxygen is formed by dissociation.

All these qualitative conclusions are confirmed by our model calculation for the gas phase chemistry following sputtering of carbon grains by OH radicals, which considers most hydrocarbons with up to four carbon atoms and a big number of reactions. The dominating sequence of reactions involved in the conversion of the hydrocarbons into CO is shown in Fig. 5.
This reaction path to a large extent is identical with the chemical pathway found to be dominating in the combustion of methane in air (e.g. Warnatz 1983, 1992). There are two major differences however: First, the hydrogen liberated in several elementary steps is not converted into H_2O as in ordinary combustion but remains due to the big hydrogen excess in the protoplanetary disk as H_2 molecule in the gas phase. The oxidation process of the carbon grains in the disk, then, resembles more closely the watergas reaction than an ordinary combustion process. Second, the direct pathway to CO from CH_2 via H_2CO and HCO is not very efficient in the protoplanetary disk but is often efficient in flames.

Our present results show that the vapourisation process (which was the carbon destruction process considered in Paper I) is completely negligible in comparison to the oxidation

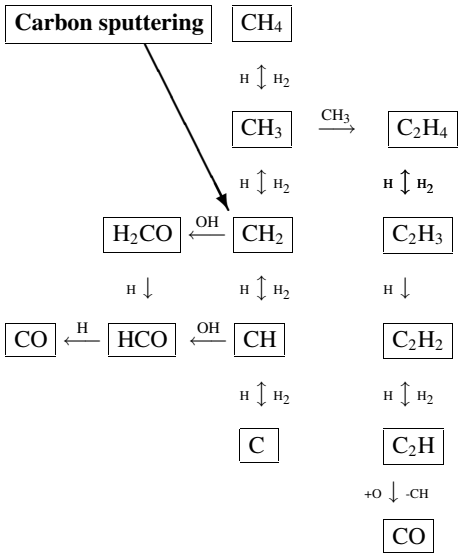

Fig. 5. The chemical pathway for CO formation following the formation of CH_2 in the reaction HCCO + H $\longrightarrow$ CO + CH_2

process since vapourisation requires a much higher temperature than oxidation.

From the intermediate products of the carbon sputtering and conversion into CO only CH_4 reaches a high abundance. From all other intermediates only CH_3 and C_2H_4 are present as temporary products with a noticeable abundance, but their abundances are lower by a factor of at least 10^3. The destruction reactions of all the gas-phase hydrocarbons are mainly oxidation reactions with the injected oxygen bearing species during olivine evaporation. The different pathways are the same with and without oxidation and can be found in Paper I. All the liberated carbon accumulates in CO until CO itself is destroyed by collisional dissociation with hydrogen. Close to the central star only free C atoms are present.

5.2. The sulfur chemistry

Troilite is the first dust component to be destroyed by the slowly heating matter. Here we assumed that it thermally decomposes at about 2 AU ($T \approx$700 K) and injects according to our assumptions only Fe and S into the gas phase. The liberated sulfur leads to a very rich chemistry between 2 and 1 AU ($T \approx$1 000 K). In order to get a better impression of the chemical composition in this region, we have shown on Fig. 6 the sulfur bearing species separately. The iron chemistry is inefficient within the frame of the neutral chemistry and we don't take it into account.

The most abundant sulfur bearing species in this region is H_2S. It forms in two very fast reactions with H_2

$$S \overset{+H_2}{\longleftrightarrow} HS \overset{+H_2}{\longrightarrow} H_2S\,. \tag{56}$$

This molecule reaches a maximum abundance of more than $10^{10}\,cm^{-3}$ between about 1.4 and 0.8 AU i.e. *where the terrestrial planets are presently located*. The Earth is just in the middle part of this region.

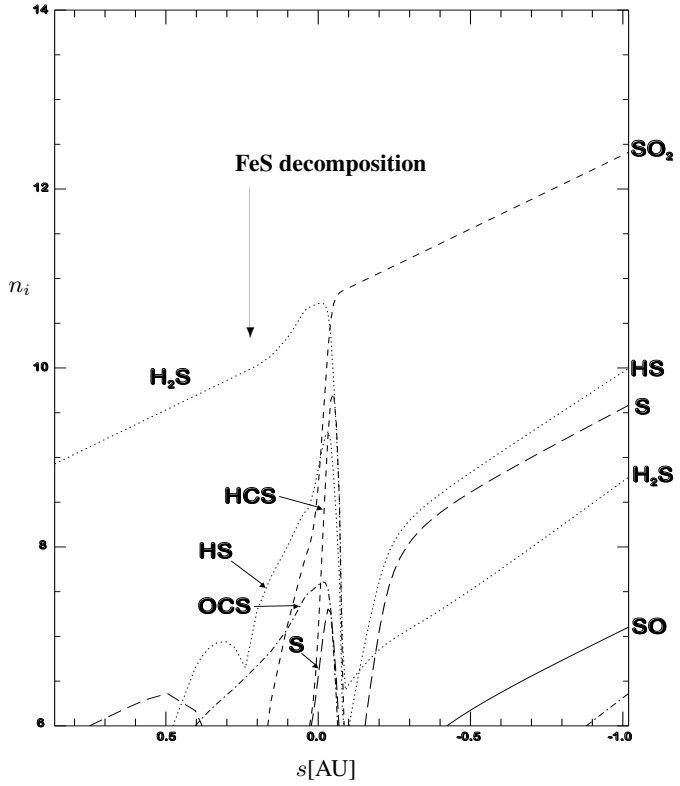

Fig. 6. Sulfur bearing species in the protoplanetary disk. One half of the total sulfur is assumed to enter the disk as gas phase H_2S. The remaining part of the sulfur is assumed to be bound in solid FeS. This S is injected into the gas phase on the decomposition of FeS at $\approx$ 2 AU.

When the olivine decomposition begins to be efficient at $\approx$0.5 AU, H_2S reacts very fast with the OH radicals and forms in a more complex reaction sequence the SO_2 molecule

$$H_2S \overset{+OH}{\longleftrightarrow} HS \overset{+O}{\longrightarrow} SO \overset{+OH}{\longleftrightarrow} SO_2\,. \tag{57}$$

Almost all the H_2S molecules are converted by this pathways into SO_2.

Other sulfur bearing species like HCS, which is quite abundant, too, are present in this domain. It forms when a free S atom reacts with a methylene radical

$$S + CH_2 \longrightarrow HCS + H\,. \tag{58}$$

Smaller amounts of OCS are produced according to the pathway

$$S \overset{+CH}{\longleftrightarrow} CS \overset{+OH}{\longrightarrow} OCS\,. \tag{59}$$

The intermediate product CS is observable in the parent molecular cloud core, in the protoplanetary disk it is efficiently converted into OCS by reaction with OH (59).

After the olivine particles are destroyed at $\approx$0.31 AU, we find besides the abundant SO_2 quite high abundances of HS and free S atoms and smaller amounts of H_2S.

In the innermost parts of the disk (see Fig. 4), the SO_2 molecules are destroyed in reactions with free oxygen atoms,

which are liberated as products of the water dissociation in this region. The pathways from SO_2 to free S atoms are

$$SO_2 \overset{+O}{\longleftrightarrow} SO \overset{+O}{\longrightarrow} S\,. \tag{60}$$

HS reacts with free O atoms, too, and forms SO, which in turn reacts with a second O atom to form a free S atom

$$HS \overset{+O}{\longleftrightarrow} SO \overset{+O}{\longrightarrow} S\,. \tag{61}$$

In the vicinity of the disk's center, only the free atoms S and Fe remain.

5.3. The silicon chemistry

The gas phase silicon chemistry is initiated when the olivine particles start to evaporate at ≈1 AU and inject SiO into the gas phase. We see from Fig. 3 that most of the Si bearing molecules in the gas phase are rare, except the SiO and the SiOOH. The latter is nearly as abundant as SiO at 0.13 AU (≈2 000 K) and below. This molecule is formed in the following reaction sequence

$$SiO \overset{+OH}{\longleftrightarrow} HSiO \overset{+OH}{\longrightarrow} SiH_2O \overset{+H_2O}{\longrightarrow} HSiOOH\,. \tag{62}$$

The SiOOH forms as dissociation product of HSiOOH

$$HSiOOH \longleftrightarrow SiOOH + H\,. \tag{63}$$

Fig. 3 clearly shows that the abundance increase of SiOOH is parallel to the abundance increase of OH. The intermediate HSiOOH is never very abundant. This result is interesting since it means that the silicon in the gas phase prior to its dissociation is not quantitatively bound in SiO as is generally assumed.

SiO_2 is present too with a low but non-negligible abundance of at most 10^{-2} of the SiO abundance. It is formed by an exchange reaction between SiO and OH

$$SiO + OH \longleftrightarrow SiO_2 + H\,. \tag{64}$$

All the silicon bearing molecules disappear in the innermost regions of the disk in the backward reactions of the above defined pathways. Due to its high bond energy SiO is the last molecule to be dissociated. The assumed process is the collisional dissociation by free H atoms and H_2 molecules

$$\begin{aligned} SiO + H &\longrightarrow Si + O + H \\ SiO + H_2 &\longrightarrow Si + O + H_2\,. \end{aligned} \tag{65}$$

The rate coefficients of these reactions are supposed to be the same as the similar carbon monoxide dissociation. Only the energy barrier must be recalculated (Paper I). As expected, only free Si atoms remain close to the central star.

6. Summary

In this work we have investigated the gas phase chemistry in a protoplanetary accretion disk including the dust destruction processes.

The usual time independent accretion disk's model has been used (Sect. 2). We calculate the chemistry in a gas parcel by solving a system of more than 100 ordinary differential equations corresponding to the different chemical species and the radii of the dust particles. The calculation is performed in the comoving frame. The chemical network is composed of about 600 chemical reactions (Sect. 3). The coupling between temperature and opacity is calculated by solving a supplementary algebraic equation (Sect. 2.1).

We have used a more realistic approximation for the gas opacity as in Paper I, where it was assumed to be constant. The mass extinction coefficients due to molecules and ions H^- have been calculated from analytical approximations to tabular values (Sect. 2.1).

Our dust model is composed of carbon (with the thermodynamical properties of graphite), olivine (Mg_2SiO_4) and troilite (FeS). We assume that these grains are embedded in two distinct layers of water and CO ice until the vapourisation temperature for CO (≈25 K) and water (≈150 K) are reached (Sect. 4).

We have considered the influence of carbon dust erosion by free O atoms and OH molecules (oxidation). This last process becomes efficient at about 2 AU. The oxidation by OH molecules modifies dramatically the hydrocarbons chemistry in the actual vicinity of the Earth by leading to the formation of huge amounts of methane. Some other hydrocarbon compounds are expected in this region to be formed but we must probably consider other types of surface reactions on grains to model their formation. The oxidation of carbon by free O atoms and the carbon vapourisation turn out to be inefficient. Methane disappears promptly because of oxidation reactions as soon as the olivine vapourisation becomes efficient (Sect. 5).

The treatment of troilite vapourisation (at ≈700 K) leads to huge densities of H_2S in the region of the terrestrial planets (between 2 and 0.8 AU). As in the case of methane, the oxygen bearing species liberated by the olivine grains oxidate H_2S, which is rapidly transformed into SO_2 (Sect. 5).

The olivine dissociation (≈1 650 K) produces SiO molecules, which lead to some other silicon bearing compounds like SiOOH or SiO_2, but the silicon chemistry has no noticeable consequences on the chemistry of the other elements (Sect. 5).

Close to the young central star (≈6 000 K), only free H, C, N, O, Mg, Fe, Si and S atoms are present.

Acknowledgements. We grateful acknowledge stimulating discussions with J. Warnatz for his hints concernig the carbon oxidation. This work has been supported by the Deutsche Forschungsgemeinschaft (DFG), Sonderforschungsbereich 359 " Reaktive Strömungen, Diffusion und Transport".

References

Alexander D.R., 1975, ApJS 29, 363

Anders E., Grevesse N., 1989, Geochimica et Cosmochimica Acta 53, 197
Bauer I., 1994, Numerische Behandlung Differentiell-Algebraischer Gleichungen mit Anwendungen in der Chemie, Master's thesis, Universität Augsburg
Bauer I., Finocchi F., Duschl W.J., Gail H.-P., Schlöder J.P., 1996, A&A 317, 273 (Paper I)
Baulch D.L., Cobos C.J., Cox R.A., Esser C., Franck P, Just Th., Ker J.A., Pilling M.J., Troe J., Walker R.W., Warnatz J., 1992, Journal of physical and chemical reference data 21, 411
Beckwith S.V.W., Sargent A.I., 1993, in Protostars and Planets III, E.H. Levy and J.I. Lunine Eds., University of Arizona Press, Tuscon, p. 521
Bell K.R., Lin D.N.C., 1994, ApJ 427, 987
Bleser G., 1986, Eine effiziente Ordnungs- und Schrittweitensteuerung unter Verwendung von Fehlerformeln für variable Gitter und ihre Realisierung im Mehrschrittverfahren vom BDF-Typ, Master's Thesis, Universität Bonn
Bontemps S., André P., Tereby S., Cabrit S., 1996, A&A 311, 858
Britten J.A., Tong J., Westbrook C.K., 1990, Twenty–Third Symposium (International) on Combustion, The Combustion Institute, p. 195
Cameron A.G.W., 1988, ARA&A 26, 441
Cassen P., 1994, Icarus 112, 405
Cronin J.R., Pizzarello S., Cruishank D.P., 1988, in Meteorites and the early solar system, J.F. Kerridge and M.S. Matthews Eds, University of Arizona Press, Tucson, p.819
Draine B.T., 1985, ApJS 57, 587
Draine B.T., Salpeter E.E., 1979, ApJ 231, 438
Draine B.T., Lee H.M., 1984, ApJ 285, 89
Duschl W.J., 1993, in: The Chemistry of Life's Origins, J.M. Greenberg, C.X. Mendoza-G'omez, and V. Pirronello Eds., Kluwer Academic Publishers, Dordrecht, p. 55
Duschl W.J., Tscharnuter W.M., 1991, A&A 241, 143
Duschl W.J., Gail H.-P., Tscharnuter W.M., 1996, A&A 312, 624 (Paper II)
Eich E., 1987, Numerische Behandlung semi-expliziter differentiellalgebraischer Gleichungssysteme vom Index 1 mit BDF-Verfahren, Master's Thesis, Universität Bonn
El-Gamal M., 1995, Thesis, University Stuttgart
Fegley Jr., B., Prinn R.G., 1989, in The Formation and Evolution of Planetary Systems, H.A. Weaver and L. Danly Eds, Cambridge University Press, Cambridge et al., p. 171
Finocchi F., Gail H.-P., 1997, A&A (accepted)
Frenklach M., Feigelson E.D., 1989, ApJ 341, 372
Garo A., Prado G., Gersum S., 1990, Combustion and Flame 79, 226
Grevesse N., Noels A., 1993, in Origin and Evolution of the Elements, N. Prantzos, E. Vangioni-Flam and M. Cassé Eds., Cambridge University Press, p. 14
Henning Th., Stognienko R., 1996, A&A 311, 291
Hudson R.L., Donn B., 1991, Icarus 94, 326
Lenzuni P., Gail H.-P., Henning Th., 1995, ApJ 447, 848
Lin, D.N.C., Papaloizou J., 1995, in Protostars and Planets II, D.C. Black and M.S. Matthews Ed., Univ. of Arizona Press, Tucson, p. 981
Lunine J.I., Stevenson D.J., 1985, ApJS 58, 493
Lunine J.I., Engel S., Rizk B., Horanyi M., 1991, Icarus 94, 333
Lynden-Bell D., Pringle J.E., 1974, MNRAS 168, 603
Mathis J.S., Rumpl W., Nordsieck K.H., 1977, ApJ 217, 425
Meyer F., Meyer-Hofmeister E., 1981, A&A 104, L 10
Millar T.J., Rawlings J.M.C., Benett A., Brown P.D., Charnley S.B., 1991, A& ASS 87, 585
Mitchell G.F., 1984, ApJS 54, 81
Neoh K.G., Howard J.B., Sarofim A.F., 1981, in Particulate Carbon Formation During Combustion, D.S. Siegla and G.W. Smith Eds., Plenum Press, New York
Neoh K.G., Howard J.B., Sarofim A.F., 1984, Twentieth Symposium (International) on Combustion, The Combustion Institute, p. 951
Neufeld D.A., Hollenbach, D.J., 1994, ApJ 428, 170
Pollack J.B., Hollenbach D., Beckwith S., Simonelli D.P., Roush T., Fong, W., 1994, ApJ 421, 615
Pringle J.E., 1996, MNRAS 281, 357
Roth P., Brandt O., von Gersum S., 1990, Twenty-Third Symposium (International) on Combustion, The Combustion Institute, p. 1485
Ruden S.P., Pollack J.B., 1991, ApJ 375, 740
Sandford S.A., Allamandola L.J., 1988, Icarus 76, 201
Sandford S.A., Allamandola L.J., 1990a, Icarus 87, 188
Sandford S.A., Allamandola L.J., 1990b, ApJ 355, 357
Sandford S.A., Allamandola L.J., 1993, ApJ 417, 815
Sharp C.M., 1992, A&AS 94, 1
Sharp C.M., Huebner W.M., 1990, ApJS 72, 417
Shull J.M., 1977, ApJ 215, 805
Swindle T.D., 1993, in Protostars and Planets III, E.H. Levy and J.I. Lunine Eds., Univ. of Arizona Press, Tucson, p. 897
Umebayashi T., Nakano T., 1981, PASJ 33, 617
van Dishoeck E., Blake G.A., Draine B.T., Lunine J.I., 1993, in Protostars and Planets III, E.H. Levy and J.I. Lunine Eds., Univ. of Arizona Press, Tucson, p. 163
van Langenvelde H.J., van Dishoeck E.F., Blake G.A., 1994, ApJ 425, L45
von Gersum S., Roth P., 1992, Twenty-Fourth Symposium (International) on Combustion, The Combustion Institute, p. 999
Warnatz J., 1983, Ber. d. Bunsengesellschaft Phys. Chem. 87, 1008
Warnatz J., 1992, Twenty-Fourth Symposium (International) on Combustion, The Combustion Institute p. 553
Wasserburg G.J., 1985, in Protostars and Planets II, D.C. Black and M.S. Matthews Eds., Univ. of Arizona Press, Tucson, p. 703
Wright I.P., Gilmour I., 1990, Nat 345, 110
Yamamoto T., 1985, A&A 142, 31

This article was processed by the author using Springer-Verlag LaTeX A&A style file *L-AA* version 3.